

Composite cation-exchange resins containing zirconium hydrophosphate for purification of water from U(VI) cations

Yuliya S. Dzyazko^a, Olga V. Perlova^b, Nataliya A. Perlova^b, Yury M. Volfkovich^{c,*},
Valentin E. Sosenkin^c, Vladimir V. Trachevskii^d, Valentina F. Sazonova^b, Alexey V. Palchik^a

^aV.I. Vernadskii Institute of General and Inorganic Chemistry of the NAS of Ukraine, Palladin Ave. 32/34, Kyiv, 03142, Ukraine

^bChemical faculty of Odesa I. I. Mechnikov National University of the MES of Ukraine, Dvoryanska Str., 2, Odesa, 65082, Ukraine

^cA.N. Frumkin Institute of Physical Chemistry and Electrochemistry of the RAS, Leninskii pr. 31, Moscow, 119071, Russia,
email: yuwolf40@mail.ru

^dTechnical Center of the NAS of Ukraine, Pokrovska Str. 13, Kyiv, 04070, Ukraine

Received 20 June 2016; Accepted 20 September 2016

ABSTRACT

Organic-inorganic ion exchangers based on strongly acidic gel-like cation exchange resin were obtained by precipitation of zirconium hydrophosphate from a $ZrOCl_2$ solution with phosphoric acid. When additionally sorbed electrolyte ($ZrOCl_2$) had been removed from the polymer before the deposition, non-aggregated particles (20–50 nm) and their aggregates (70–300 nm) were formed in voids between gel regions of the polymer. Particles of micron size were precipitated from additionally sorbed electrolyte in structure defects. The inorganic constituent in these pores is characterized by the highest content of phosphorus. As it was found with a method of standard contact porosimetry, the largest particles increase swelling pressure: formally they can be considered to be a cross-linking agent. However, they increase effective diffusion coefficient of $UO_2^{2+} \rightarrow H^+$ exchange from 0.66×10^{-12} up to $1.73 \times 10^{-12} \text{ m}^2 \text{ s}^{-1}$. As a result, this ion-exchanger is the most effective for removal of UO_2^{2+} species from water containing also hardness ions. Regarding the samples containing smaller particles, $UO_2^{2+} \rightarrow H^+$ exchange is complicated by chemical interaction of sorbed ions with functional groups of the inorganic constituent. Sorption isotherms are described by the Dubinin–Radushkevich model. Transformation of porous structure of the polymer due to zirconium hydrophosphate was shown to affect UO_2^{2+} sorption by the composites.

Keywords: Uranium(VI); Ion exchange; Organic-inorganic ion-exchanger; Zirconium phosphate; Standard contact porosimetry

1. Introduction

Uranium is a widespread chemical element – its content is $\approx 3 \mu\text{g g}^{-1}$ both in lithosphere (mainly in rocks with high silicon content) [1] and in sea water [2]. Significant uranium content in water sources is explained by the ingress of mine water, wastes of nuclear power plants, mining and mineral processing plants.

Maximum permissible concentration for uranium in a form of soluble compounds is 0.015 mg dm^{-3} , even lower values are recommended [3] due to radioactivity and toxicity of this element. Uranium as well as its decay products affects all cells of living organisms, the poisoning leads to pathology of different organs and systems (especially kidneys), accumulation of uranium causes radiation sickness. Thus, uranium removal from water is important practical task.

Well-known technique for uranium removal from water is chemical [4] or photocatalytic [5] reduction of U(VI) to

*Corresponding author.

Presented at the EDS conference on Desalination for the Environment: Clean Water and Energy, Rome, Italy, 22–26 May 2016.

U(IV) (transformation of soluble compounds into UO_2). These methods require significant amount of reagents (hydrogen sulphide, alkyl sulphides etc.); thus, the problem of secondary wastes arises. Biological methods of uranium reduction are developed now [6]. However, in order to decrease a content of U(VI) compounds in water down to the maximum permissible concentration, tertiary treatment is necessary. Adsorption and ion exchange are effective methods for the solution of this problem [7–18]. The sorbent has to be regenerated easy and completely, the uranium-containing effluent can be used further in technological operations of uranium ore processing. In owing to this, ion-exchange resins [7,9,10,13–16] or inorganic ion exchangers like amorphous zirconium hydrophosphate (ZHP) have been proposed [17,18].

Nevertheless, the efficiency of ion exchange processes is limited by low selectivity of strongly acidic or strongly basic ion exchange resins, which demonstrate high sorption rate and sorb U(VI) compounds from solutions of wide pH diapason [9,15]. In order to overcome these difficulties, the resins are modified with inorganic sorbents [13] or lignocellulose [16]. A method of molecular imprinting is also used [14]. Chelate resins [10] and inorganic phosphate-containing ion-exchangers [17,18] possess significant selectivity towards U(VI) ions. However, a rate of sorption is rather slow mainly due to complex formation of species with functional groups of the inorganic sorbents, resins or their modifiers.

As known, small ZHP particles incorporated into ion exchange resins provide fast sorption of Cd^{2+} [19–21] and

Ni^{2+} [21–23] ions as well as considerable capacity of the composites towards these species during their removal from solutions containing also hardness ions and organics [19–22]. The materials have been recommended for ion exchange [19,21,22] and electrodeionization [20,22]. Inorganic particles transform porous structure of the polymer constituent and affect functional properties of the composites [19–24]. The purpose of this work is to establish the interrelation between structure of the ZHP-containing composites and sorption of U(VI) ions. Another tasks are to ascertain a possibility to remove U(VI) compounds from water and to use the ion-exchangers many times.

2. Experimental

2.1. Ion-exchangers

Such strongly acidic cation-exchanger as Dowex HCR-S (Dow Chemical) containing $\approx 8\%$ DVB was used for modification. Its ion exchange ability is provided by $-\text{SO}_3\text{H}$ groups. In opposite to [25–27], the resin is related to gel-like materials. Preliminarily the resin was washed with NaOH, HCl solutions and deionized water as described elsewhere.

As seen from Fig. 1, the modification procedure involved following stages: (i) washing of weighted amount of the resin with acetone (to remove unpolymerized organics) and drying at room temperature; (ii) swelling in deionized water; (iii) impregnation with a 1 M ZrOCl_2 solution for 24 h followed by separation of solid

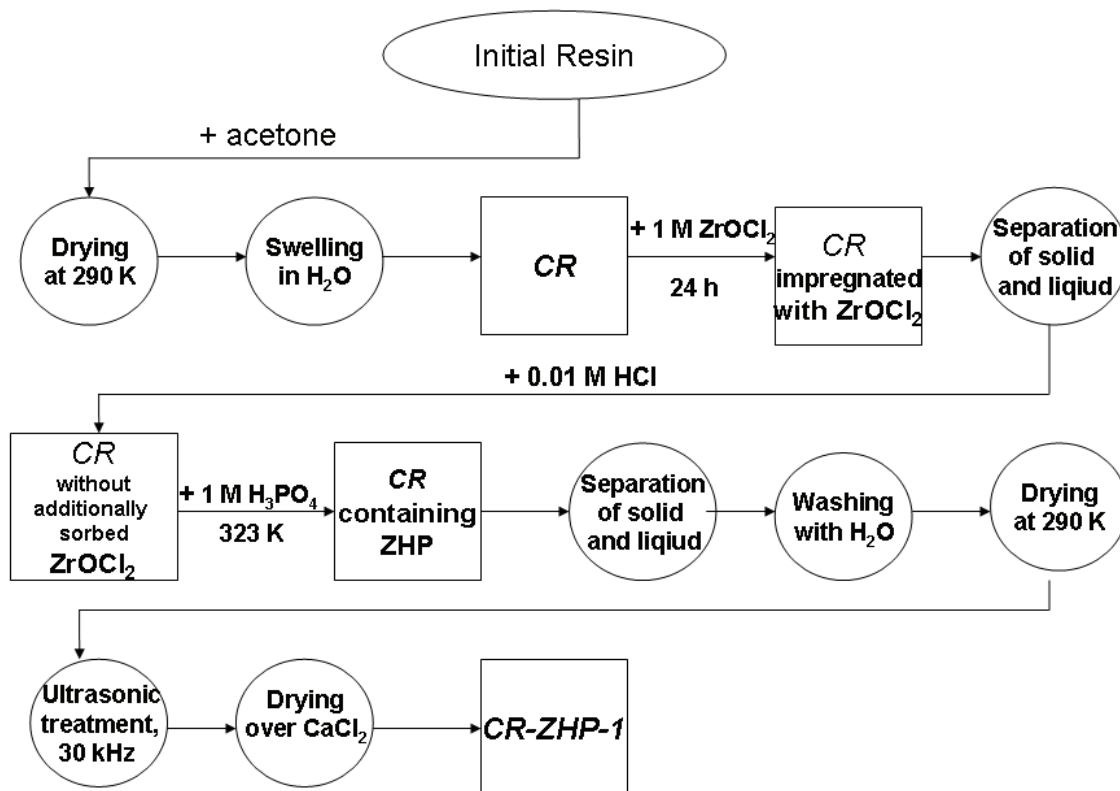


Fig. 1. Synthesis of the CR-ZHP-1 sample.

and liquid; (iv) washing with a 0.01 M HCl solution for removal of additionally sorbed electrolyte; (v) treatment with a 1 M H_3PO_4 solution at 323 K, separation of the solid and liquid, washing of the resin with deionized water up to pH 7 of the effluent; (vi) drying at room temperature followed by a treatment with ultrasound at 30 kHz using a Bandelin ultrasonic bath (Bandelin, Hungary); (vii) drying in a desiccator over CaCl_2 at 293 K down to constant mass. The differences of this technique from [19,20,22–24] is ZHP precipitation under elevated temperature and use of zirconium-containing solution instead of sol [21] for the resin impregnation.

The (ii)–(vii) stages were repeated one or seven times, the samples were marked as *CR-ZHP-1* and *CR-ZHP-3*, respectively. The pristine resin washed with acetone was also investigated for a comparison (*CR*). The *CR-ZHP-2* sample was obtained by similar manner as *CR-ZHP-1*, but the (iv) stage was excluded. Individual inorganic exchanger (marked as *ZHP*) was also synthesized by means of a mixing of ZrOCl_2 and H_3PO_4 solutions followed by immediate dispersion of the precipitate in the column filled with a nonpolar liquid as described in [28]. The ion-exchanger was sieved; a fraction of 0.5–1 mm was taken.

A size of air-dry grains was determined using a Crystal-45 optical microscope (Konus, USA). 300 particles for each sample were analyzed. The particle size distributions were plotted as dependencies of particle fraction (W) on grain radius (\bar{r}_g). The W value was calculated according to the expression:

$$W_i = \frac{q_i}{\sum_{i=1} q_i} \quad (1)$$

where q is the amount of particles of one or the other size, i is the integer $\left(\sum_{i=1} q_i = 300\right)$.

2.2. Visualization of ZHP and porosity measurements

TEM images were obtained by means of a JEOL JEM 1230 transmission electron microscope (Jeol, Japan). Preliminarily the ion-exchangers were milled and treated with ultrasound.

A method of standard contact porosimetry (SCP) [29–31], which has been recognized by the IUPAC [32], was applied to the unmodified resin and composites as described, for instance, in [20]. Preliminarily the samples were heated at 353 K under vacuum and impregnated with deionized water. An equilibrium curve of relative moisture content at 293 K was determined for the sample, the pore size distributions and isotherms of water desorption were plotted.

2.3. Chemical composition

The content of phosphorus and zirconium in the samples was analyzed with a X-Supreme8000 XRF (X-ray fluorescence) spectrometer (Oxford Instruments, UK). NMR ^{31}P spectra were obtained with an AVANCE 400 spectrometer (Bruker, Germany) using single-pulse technique under the accumulation mode at 162 MHz, chemical shift was determined relatively to 85% H_3PO_4 .

2.4. Uranium sorption under batch conditions

The experiments were carried out at 296 K. A $\text{UO}_2\text{Ac}_2 \cdot 2\text{H}_2\text{O}$ salt (Chemapol, Czech Republic) was used for preparation of solutions, which contained also HCl (0.02 M, pH 2.5). This acid is used for treatment of uranium-containing minerals, such as monazite [33].

When a rate of ion exchange was investigated, the initial concentration of U(VI) was 2×10^{-4} M. For each ion-exchanger, a series of weighted samples (0.1 g) was prepared, inserted to flasks, where aliquots of the solution were added (50 cm^3). As found preliminarily, this is a minimal dosage of the ion-exchangers, which provides the most complete U(VI) removal. The process was carried out under intensive stirring by means of a Water Bath Shaker Type 357 (Elpan, Poland). After predetermined time, the solid and liquid from one flask were separated, after the next period the solution was removed from the second flask and so on. U(VI) ions were transformed into a complex with Arsenazo III, the solution was analyzed using a Shimadzu UV-mini1240 spectrophotometer (Shimadzu, Japan) at 670 nm [34]. Sorption capacity (A) was determined as:

$$A = \frac{V_s(C_i - C_t)}{m} \quad (2)$$

where C_i and C_t are the initial concentration and concentration after certain time, respectively, V_s is the solution volume, m is the sorbent mass.

Solutions of various U(VI) concentration (from 1×10^{-5} M to 2×10^{-4} M) containing also HCl were used for obtaining of sorption isotherms. Other conditions were similar to those described above. The pH value under equilibrium state was controlled with a I-160-MI pH-meter (Izmeritel'naya Technika, Ltd, RF).

2.5. Uranium sorption under dynamic conditions

The solution containing U(VI) (2×10^{-4} M) and HCl (0.02 M) was prepared using tap water, where Ca^{2+} (1.7×10^{-3} M) and Mg^{2+} (1×10^{-3} M) ions were present. A diameter of the column was 0.7 cm, a height of the ion-exchanger bed was 5 cm, the solution velocity was 5 $\text{cm}^3 \text{min}^{-1}$. The effluent at the column outlet was analyzed as mentioned above.

2.6. Regeneration of ion-exchanger and its multiple usage

The ion-exchanger that was loaded in the column (as described in Section 2.5) was regenerated under dynamic conditions by passing of a 0.1 M H_2SO_4 solution with a velocity of 1 $\text{cm}^3 \text{min}^{-1}$. Regeneration degree (R_d) towards U(VI) was calculated from the formula:

$$R_d = \frac{V_d C_d}{Am} \times 100\% \quad (3)$$

where C_d and V_d are the concentration and volume of the effluent, respectively.

A weighted sample (0.1 g) of ion-exchanger, which had been loaded preliminarily with a 2×10^{-4} M U(VI)-containing solution (50 cm^3), was regenerated with a 1 M H_2SO_4

solution (50 cm³) under batch conditions. The regeneration degree was calculated as:

$$R_d = \frac{C_d}{C_i - C_{eq}} \times 100\% \quad (4)$$

where C_{eq} is the equilibrium concentration of the solution after sorption.

After regeneration, the ion-exchanger was washed with deionized water, dried and used again. The procedure of sorption-regeneration was repeated several times.

3. Results

3.1. Morphology and chemical composition of the inorganic constituent

Incorporated particles cause an increase of size of resin grains (Fig. 2). The most significant change has been found for the CR-ZHP-2 sample, which contains the highest mass fraction (m) of ZHP. In this case, the inorganic constituent was deposited from the additionally sorbed $ZrOCl_2$ solution. An average particle radius (\bar{r}_g) is given in Table 1.

As seen for the CR-ZHP-1 and CR-ZHP-3 samples, both non-aggregated ZHP particles (20–50 nm) and their aggregates (70–300 nm) are formed in the resin during modification (Fig. 3). The CR-ZHP-2 ion-exchanger contains not only aggregates, but also large dendritic agglomerates.

Smaller non-aggregated ZHP nanoparticles (4–20 nm) have been found for the composites obtained under room [19,22,24] and lower [20] temperature. Under elevated

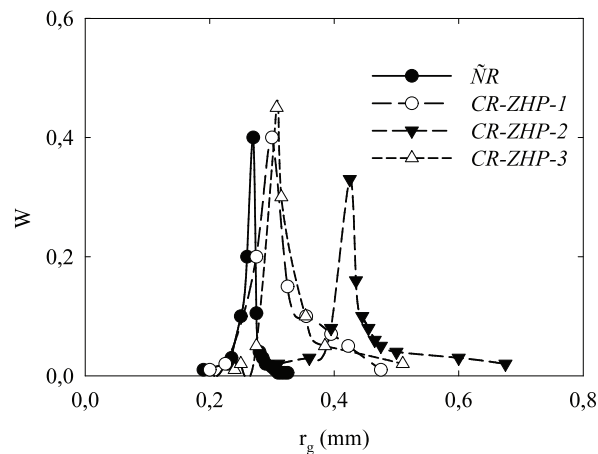


Fig. 2. Grain size distributions.

Table 1
Characteristics of ion-exchangers

Sample	$\bar{r}_g \times (m)$	m	Molar ratio		$P/P_s (A_{H_2O} = 0.75 \text{ cm}^3\text{g}^{-1})$	A_{H_2O} for transport pores (cm^3g^{-1})	n
			Zr:P	$-OPO_3H_2:(-O)_2PO_2H$			
CR	2.65 ± 0.01	0	–	–	0.55	0.73	8.4
CR-ZHP-1	3.15 ± 0.01	0.10	1:0.3	1:1.50	0.43	0.76	9.8
CR-ZHP-2	4.40 ± 0.02	0.50	1:0.43	1:1.20	0.43	0.63	14.6
CR-ZHP-3	3.20 ± 0.01	0.15	1:0.25	1:0.85	0.82	0.80	10.9
ZHP	3.75	1	1:1.44	1:0.95	–	–	–

temperature (T), the smallest ZHP particles are dissolved during precipitation, larger particles are re-deposited in accordance with Ostwald–Freundlich equation [35]:

$$\ln \frac{C_{ZHP}}{C_{ZHP,s}} = \frac{\beta v_m \sigma \cos \phi}{RT r_p} \quad (5)$$

where C_{ZHP} and $C_{ZHP,s}$ are the concentration of dissolved ZHP and its saturated solution, respectively (these values are extremely low), β is the shape factor of particles, v_m is the molar volume of ZHP, σ is the surface tension of the solvent, ϕ is the wetting angle (≈ 1 for hydrophilic ZHP), R is the gas constant, r_p is the radius of incorporated particles.

Typical NMR ³¹P spectra includes two signals (Fig. 4). As known for crystalline ZHP, the signal of $(-O)_2PO_2H$ groups (α -modification) is displaced upfield relatively to that for $-OPO_3H_2$ groups (γ -ZHP) [36]. The CR-ZHP-1 sample shows the highest molar ratio of $-OPO_3H_2$ and $(-O)_2PO_2H$ groups, the lowest ratio has been found for the CR-ZHP-3 ion-exchanger.

3.2. Isotherms of water adsorption

Earlier the SCP technique data were applied to investigation of porous structure of rigid (ceramics [37], carbon [38]) and polymer [19–21,23,24,39,40] materials. The method allows us to analyze only the polymer constituent, since the thermal pretreatment cannot provide complete water removal from ZHP.

A slow growth of water adsorption (A_{H_2O}) in a wide interval of P/P_s (here P is the pressure of water vapor, P_s is the pressure of saturated vapor) is related to micropores and partially to mesopores (Fig. 5). The vertical region at $P/P_s \rightarrow 1$ is attributed to meso and macropores.

A change of the swelling pressure, which is defined in the framework of Gregor's model [41], can be estimated qualitatively by a comparison of the P/P_s ratios at similar A_{H_2O} values (see Table 1). The aggregates of ZHP particles reduce the swelling pressure in the polymer (CR-ZHP-1, CR-ZHP-3). At the same time, the agglomerates increase the swelling pressure (CR-ZHP-2).

3.3. Porous structure of the pristine resin

Porous structure of polymer gel-like ion exchange materials is formed only during swelling. The structure involves several types of pores, which contain functional groups (channels, clusters, they are so called transport pores) and free from them (voids between gel regions, structure defects)

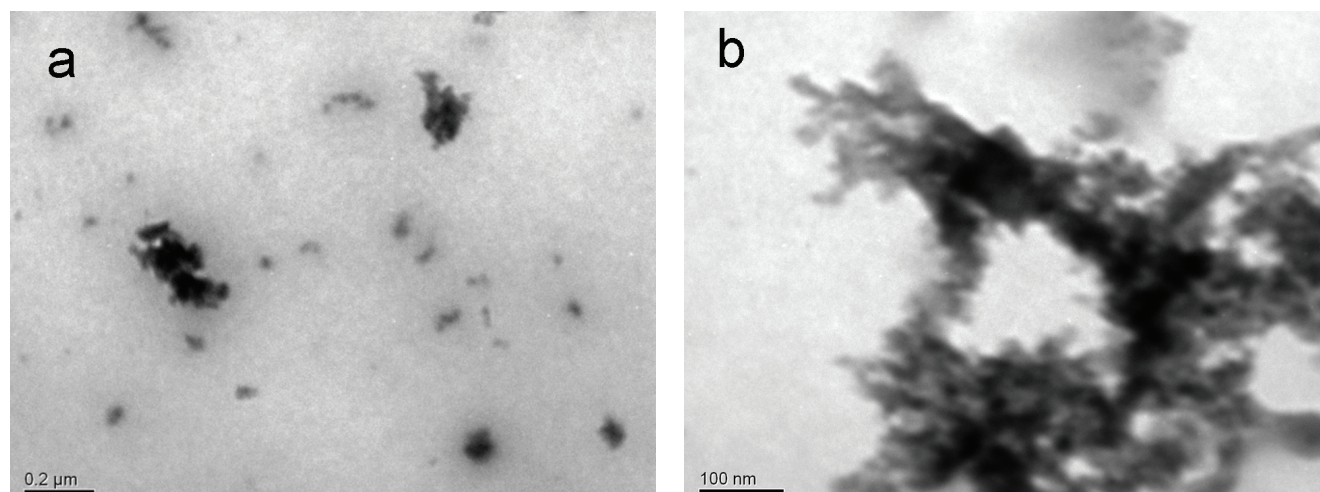


Fig. 3. TEM images of ZHP particles in the CR-ZHP-1 (a) and CR-ZHP-2 (b) samples.

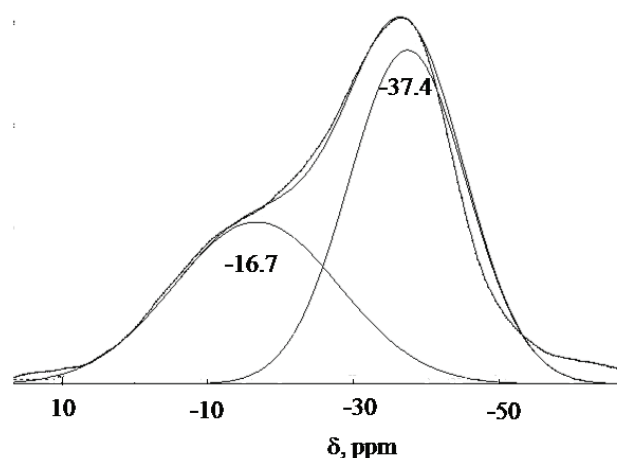


Fig. 4. Typical NMR ^{31}P spectra for ZHP-containing composite (CR-ZHP-1).

Note: Signals at ≈ -17 and ≈ -37 ppm are attributed to $-\text{OPO}_3\text{H}_2$ and $(-\text{O})_2\text{PO}_2\text{H}$ groups, respectively.

[39,42]. Integral pore size distribution for the pristine resin is plotted in Fig. 6(a) as a dependence of pore volume (V) on a logarithm of pore radius (r). The volume of micropores (channels) corresponds to intersection of integral curves with the ordinate axes.

Fig. 6(b) illustrates differential distribution, one or another types of pores were recognized according to review [42] and also experimental papers [19–21,23,24,39,40]. Regarding the pristine ion-exchanger, peaks at $\log r = 0.46$ (nm) and 0.63 (nm) are attributed to clusters and voids between gel regions, respectively. A volume of pores that correspond to plateau of the integral distribution ($\log r = 0.6\text{--}2$ (nm)) is $0.06 \text{ cm}^3 \text{ g}^{-1}$. It means that the voids between gel regions are available for ZHP particles during modification; clusters are free from the inorganic constituent. A small peak at $\log r = 3.5$ (nm) is related to structure defects. Further increase of water content is due to both large structure defects and voids between ion-exchanger grains.

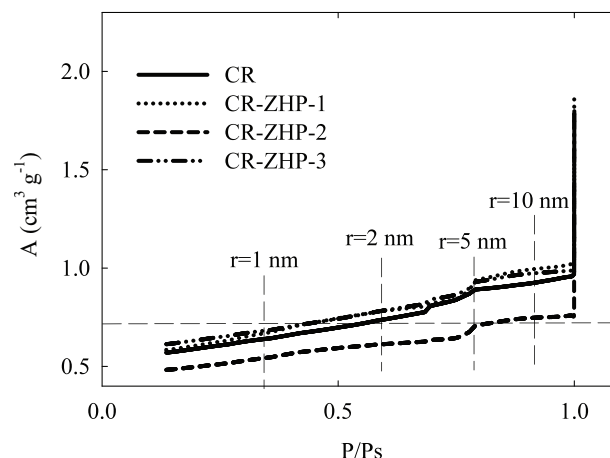


Fig. 5. Isotherms of water adsorption.

Note: Vertical dashed lines correspond to pores of certain size, horizontal line indicates water adsorption of $0.75 \text{ cm}^3 \text{ g}^{-1}$.

We can calculate a number of water molecules (n) in a hydration shell of counter-ions (H^+) of $-\text{SO}_3\text{H}$ groups (see Table 1) as:

$$n = \frac{A_{\text{H}_2\text{O}}}{A_p V_{\text{H}_2\text{O}}} \quad (6)$$

where A_p is the exchange capacity of the polymer ($4.8 \text{ mg-equ g}^{-1}$). The $A_{\text{H}_2\text{O}}$ value is the content of water in clusters and channels, $V_{\text{H}_2\text{O}}$ is the molar volume of water. As a rule, hydration shells are incomplete due to a small distance between functional groups [41].

3.4. Composites: porous structure of the polymer constituent

Small aggregates of ZHP nanoparticles, which can be located in voids between gel regions (CR-ZHP-1 and CR-ZHP-3), cause a shift of the peaks to the region of lower $\log r$ values for clusters and void between gel regions, respectively (see Fig. 6). Regarding the CR-ZHP-1 sample,

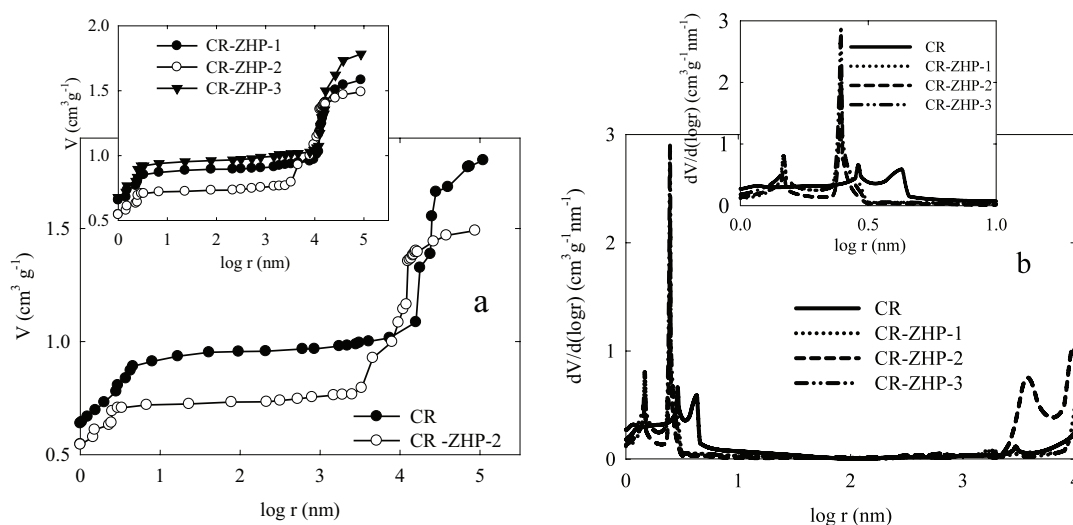


Fig. 6. Integral (a) and differential (b) pore size distributions obtained with a SCP method.

a volume of pore is $0.05 \text{ cm}^3 \text{ g}^{-1}$ within the diapason of $\log r = 0.5\text{--}2$ (nm). It means a possibility of ZHP deposition in these pores after one-time modification of the polymer. In the case of *CR-ZHP-2*, the peaks for clusters and voids between gel regions occupy the same positions.

The aggregates, which are evidently located in voids between gel regions, are a barrier against co-ions. During further modification of the *CR-ZHP-1* sample, they prevent penetration of phosphate anions inside the grains. As a result, the *CR-ZHP-3* ion-exchanger is characterized by the lowest content of phosphorus (see Table 1).

According to a size of the agglomerates (*CR-ZHP-2*), they are located in structure defects and increase their volume. These pores are evidently more available for counter-ions during ZHP precipitation. Thus, the highest content of phosphorus has been found for this composite.

The n values were calculated via the formula:

$$n = \frac{A_{\text{H}_2\text{O}}}{A_p V_{\text{H}_2\text{O}} (1 - m)} \quad (7)$$

A growth of ZHP content causes an increase of this parameter evidently due to increase of the distance between functional groups and, as a result, completion of hydration shells of counter-ions.

The α and γ parameters (Fig. 7) have been proposed earlier [19–21,40] in order to estimate transformation of the polymer pores. The α parameter is a volume ratio of transport and non-transport pores. The γ value is a volume ratio of pores containing bounded water ($r < 1.5 \text{ nm}$ [42]) and pores filled also with free water ($r > 1.5 \text{ nm}$).

Regarding the pristine resin, Gregor's swelling pressure is caused by fixed and counter-ions of $-\text{SO}_3\text{H}$ groups in clusters and channels. This value is too high ($\approx 1.5 \times 10^7 \text{ Pa}$ for materials of this type [41]). In the case of composites, osmotically active species are located also in pores, which are free from functional groups. Channels and clusters play a role of a semi-permeable separator. ZHP particles squeeze these pores due to swelling pressure from the side of larger pores (decrease of the α parameter and increase of the γ value,

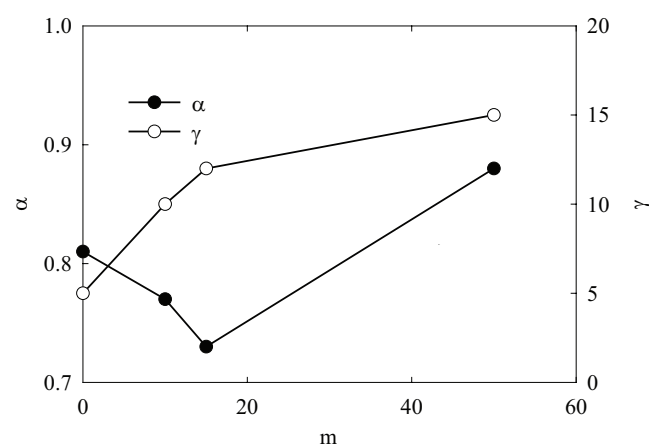


Fig. 7. The α and γ parameters as functions of ZHP mass fraction.

compare *CR*, *CR-ZHP-1* and *CR-ZHP-3*). A size of clusters and channels decreases, a part of them is unavailable for water. The *CR-ZHP-1* and *CR-ZHP-3* samples show lower swelling pressure than the pristine resin.

The agglomerates of micron size (*CR-ZHP-2*) squeeze both the transport pores and voids between gel regions (increase of the α and γ parameters). They reinforce total swelling pressure due to osmotically active species in structure defects. Squeezing causes stretching of the polymer chains (unwinding of macromolecule coil), the distance between $-\text{SO}_3\text{H}$ groups increases, the hydrate shells of H^+ ions become more complete.

3.5. Rate of ion exchange

UO_2^{2+} species dominate in a medium of hydrochloric acid at pH 2.5 [43]. Fractional attainment of equilibrium (F) on time (t) is plotted in Fig. 8 ($F = A_t/A_\infty$, where A_t and A_∞ are the capacity after certain time and under equilibrium conditions, respectively).

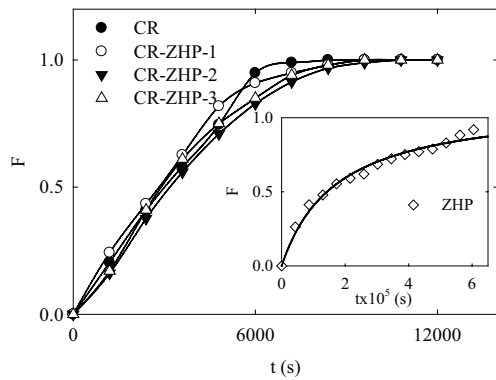


Fig. 8. Dependencies of fractional attainment of ion exchange equilibrium on time.

If the limiting stage of sorption is particle diffusion, it is valid [41]:

$$F = [1 - \exp(\pi^2(f_1(\alpha)\tau + f_2(\alpha)\tau^2 + f_3(\alpha)\tau^3))]^{0.5} \quad (8)$$

for exchange of ions with different mobility. Here, $\alpha = \bar{D}_{A^{++}} / \bar{D}_{B^+}$, \bar{D} is the self-diffusion coefficient (for isotope exchange), UO_2^{2+} and H^+ are designated as A^{++} and B^+ , $\tau = \frac{\bar{D}_{A^{++}} t}{r_s^2}$. It means:

$$\ln(1 - F^2) = \pi^2(f_1(\alpha)\tau + f_2(\alpha)\tau^2 + f_3(\alpha)\tau^3) \quad (9)$$

The $\ln(1 - F^2) - t$ plot is fitted with a cubic polynomial (Fig. 9(a), Table 2). High correlation coefficients (R^2) point particle diffusion as, at least, one rate-determining stage.

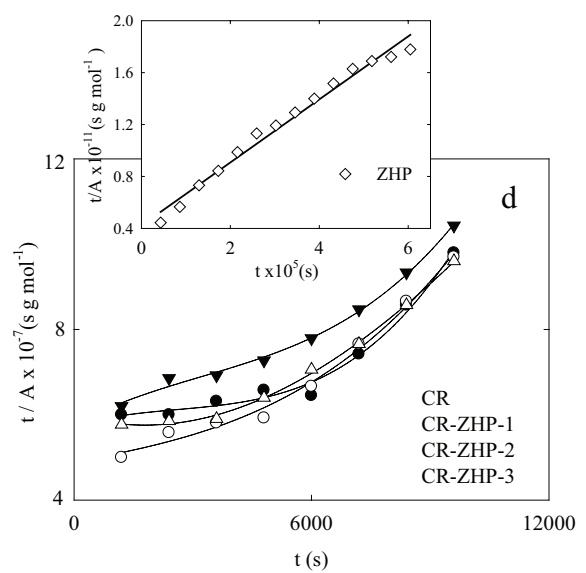
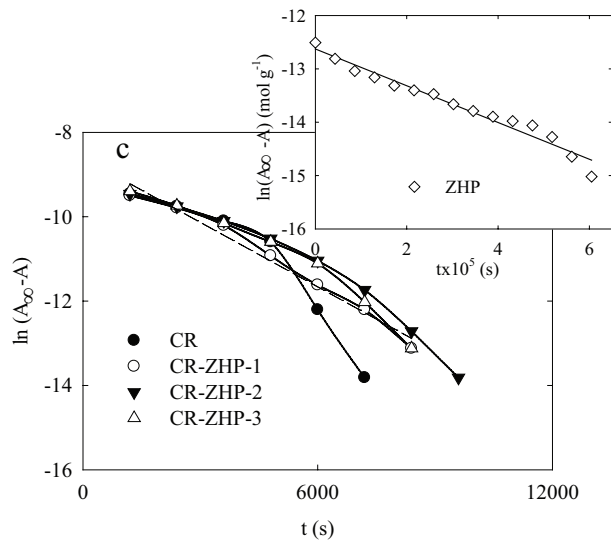
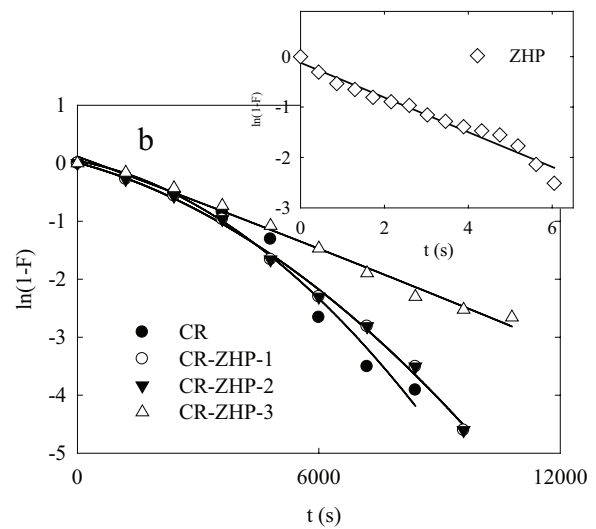
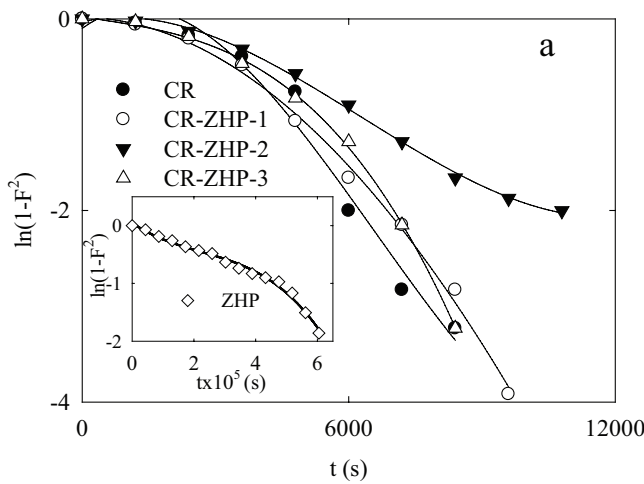


Fig. 9. Modeling of $UO_2^{2+} \rightarrow H^+$ exchange on polymer and organic-inorganic resins. Note: Insertions: it is the same for ZHP. Following models were used: particle diffusion (a), film diffusion or chemical reaction (b), reactions of pseudo-first (c) and pseudo-second-order (d).

Table 2
Modeling of U(VI) sorption rate

Sample	A_∞ (mmol g ⁻¹)	Cubic polynomial (particle diffusion)			Linear polynomial, R^2		
		R_c^2	$t_{1/2}$ (s)	$\bar{D}_{A^{++}, B^+} \times 10^{12}$ (m ² s ⁻¹)	Film diffusion or reaction	Reaction of pseudo-first-order	Reaction of pseudo- second-order
CR	0.098	0.97	3,180	0.66	0.93	0.88	0.81
CR-ZHP-1	0.099	0.99	2,940	1.01	0.97	0.98	0.93
CR-ZHP-2	0.093	0.99	3,360	1.73	0.97	0.94	0.94
CR-ZHP-3	0.100	0.99	3,120	0.98	0.99	0.95	0.91
ZHP	0.034	0.99	145,000	0.03	0.96	0.96	0.98

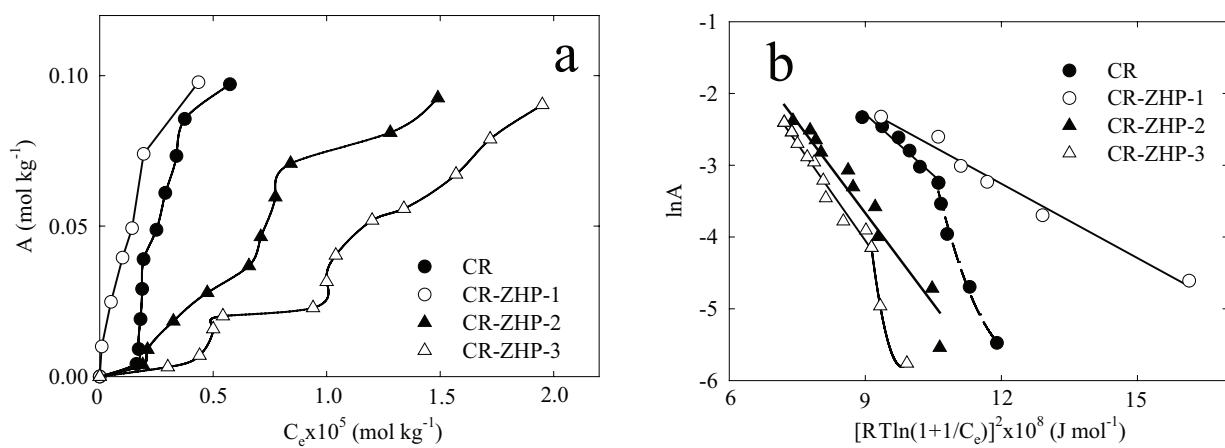


Fig. 10. Isotherms of UO₂²⁺ sorption (a) and their linearization according to the D-R model (b).

Effective diffusion coefficient (\bar{D}_{A^{++}, B^+}), which is related to $A^{++} \rightarrow B^+$ exchange, is determined from the expression [41]:

$$\bar{D}_{A^{++}, B^+} = 0.03 \frac{\bar{r}_g^2}{t_{1/2}} \quad (10)$$

where $t_{1/2}$ is the half-time of exchange.

The \bar{D}_{A^{++}, B^+} value depends on self-diffusion coefficients of both A^{++} and B^+ ions and their content in the ion-exchanger. Under low content of A^{++} species, the effective diffusion coefficient is close to $\bar{D}_{A^{++}}$. The highest effective diffusion coefficient has been found for the CR-ZHP-2 sample, the inorganic ion-exchanger is characterized by the lowest value.

In the case of film diffusion, the $\ln(1 - F)$ value is proportional to time [44], when ions of equal mobility are exchanged. Since the experiments were performed in acidic solution containing low amount of U(VI) cations, it is assumed no significant change of H⁺ concentration at the solid-liquid interface. It means no influence of H⁺ ions on the rate of ion exchange. However, linearity of $\ln(1 - F) - t$ plot can indicate also chemical reaction as a rate-determining stage [44]. As seen from Fig. 9(b) and Table 2, the $\ln(1 - F) - t$ plot can be linearized satisfactorily only for the CR-ZHP-3 sample and ZHP. Owing to lower \bar{D}_{A^{++}, B^+} values for these samples in a comparison with other ion-exchangers, the linearity can be related rather to chemical reaction.

The model of pseudo-first-order is described by the Lagergren equation [45]:

$$\ln(A_\infty - A) = \ln A_\infty - K_1 t \quad (11)$$

The model of pseudo-second-order proposed by Ho and McKay is as follows [46]:

$$\frac{t}{A} = \frac{1}{K_2 A_\infty^2} + \frac{1}{A_\infty} \cdot t \quad (12)$$

where K_1 and K_2 are the rate constants.

The model of pseudo-first-order (Fig. 9(c)) can be applied only to the CR-ZHP-1 sample ($K_1 = 4.7 \times 10^{-4} \text{ s}^{-1}$), the model of pseudo-second-order (Fig. 9(d)) is valid only for ZHP ($K_2 = 1.9 \times 10^{-4} \text{ dm}^3 (\text{mmol s})^{-1}$). Thus, the rate of UO₂²⁺ sorption is complicated by chemical reaction for the CR-ZHP-1, CR-ZHP-3 and ZHP samples. This can be caused by partial exclusion of -SO₃H groups from ion exchange. The reaction can be deposition of insoluble U(VI) compounds [18] or complex formation similarly to 3d metals [47]. Despite the reaction, the \bar{D}_{A^{++}, B^+} coefficient decreases in the order: CR-ZHP-1 ≥ CR-ZHP-3 > CR. The diffusion coefficient is determined as l^2/τ , where l is the distance between functional groups, τ is the relaxation time. Higher sorption rate

on the composites is evidently due to increase of the distance between $-\text{SO}_3\text{H}$ groups.

The CR-ZHP-2 ion-exchanger behaves similarly to the pristine resin: the sorption rate is determined mainly by the polymer. Despite the inorganic constituent, this ion exchanger shows the highest D_{A^{++}, B^+} value evidently due to the largest distance between functional groups (the highest n magnitude has been found this sample).

3.6. Sorption isotherms

Isotherms of UO_2^{2+} sorption are given in Fig. 10(a). The plots for the CR-ZHP-1 and CR-ZHP-3 samples show the most rapid and the slowest build-up, respectively. The pH of the equilibrium solution was found to be lower in a comparison with the initial solution: a shift was from 2.5 down to 2.2 (CR and CR-ZHP-2). In the case of CR-ZHP-1 and CR-ZHP-3, a slight shift towards larger values has been found.

The Langmuir, BET, Freundlich and Dubinin–Radushkevich (D-R) models [48] were applied to the isotherms. Linearization according to the first 3 models gave either no straight lines (Langmuir, BET) or unreasonable coefficients (the exponent value of the Freundlich model was higher than 1). The D-R model:

$$\ln A = \ln A_{\text{DR}} - \frac{R^2 T^2}{E^2} [\ln(1 + 1/C_e)]^2 \quad (13)$$

has been found to give linear approximation within a certain interval of concentration of equilibrium solution (Fig. 10(b)). Here A_{DR} corresponds to total exchange capacity, E is the adsorption energy. The D-R approach provides full filling of micropores with adsorbate. Large UO_2^{2+} ions occupy whole volume of micropores within the interval of exchange capacity, where the D-R equation is valid (Table 3).

Table 3
Parameters for the D-R isotherms

Sample	Interval of $A \times 10^2$, (mol kg ⁻¹)	R_c^2	E (kJ mol ⁻¹)	$\ln A_{\text{DR}}$
CR	3.90–9.71	0.97	13.37	2.80
CR-ZHP-1	1.00–9.78	0.98	15.91	0.88
CR-ZHP-2	0.89–9.26	0.97	10.91	3.92
CR-ZHP-3	1.58–9.03	0.97	10.54	4.05

Table 4
 UO_2^{2+} removal from combining solution and regeneration of the sorbents under dynamic conditions

Sample	V_s/V_i (corresponds to breakthrough capacity)	Breakthrough capacity towards U(VI)		R_d (%) at $V_s/V_i = 10$
		mmol g ⁻¹	mmol cm ⁻³	
CR	2.9	7.47×10^{-4}	3.4×10^{-4}	50
CR-ZHP-1	3.4	1.42×10^{-3}	7.12×10^{-4}	58
CR-ZHP-2	11.3	3.79×10^{-3}	2.36×10^{-3}	87
CR-ZHP-3	1.80	6.68×10^{-4}	3.93×10^{-3}	65

Modification of the resin causes a shift of lower boundary of this interval towards smaller A values. The energy magnitudes indicate preferable ion exchange mechanism (normally this diapason is of 8–16 kJ mol⁻¹) [48]. Too high A_{DR} values for all samples (except CR-ZHP-1) are evidently due to heterogeneous distribution of functional groups in pores. Their density per unit of surface area is obviously higher in micropores, which are fully occupied with UO_2^{2+} species, than in other pores. A size of these micropores is comparable with that for sorbed ions.

A size of some transport pores becomes comparable with that of UO_2^{2+} ions providing validity of the D-R model within a wide interval of sorption capacity. In the case of the composites, this can be caused also by ZHP. A growth of the γ and A_{DR} parameters (CR → CR-ZHP-1 → CR-ZHP-3, CR → CR-ZHP-2) indicates formation of these sorption centers.

3.7. Sorption under dynamic conditions

Despite practically similar sorption capacity for both CR and composites in a 2×10^{-4} M UO_2^{2+} solution (see Table 2), the highest value of breakthrough capacity is reached for the CR-ZHP-2 sample (Fig. 11, Table 4). This is evidently due to fast exchange on the one hand and high content of micropores, which can be considered as centers of selective sorption. Indeed, this sample shows the highest D_{A^{++}, B^+} and $\ln A_{\text{DR}}$ values.

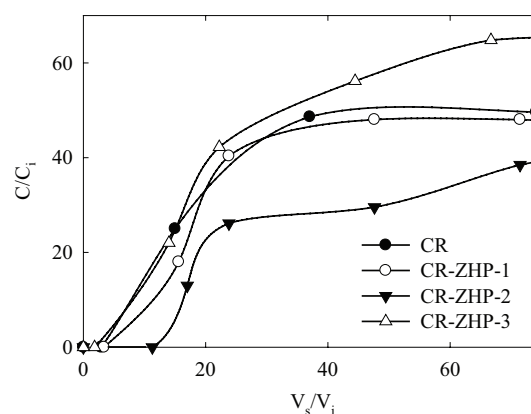


Fig. 11. UO_2^{2+} removal from a combining solution containing also hardness ions.

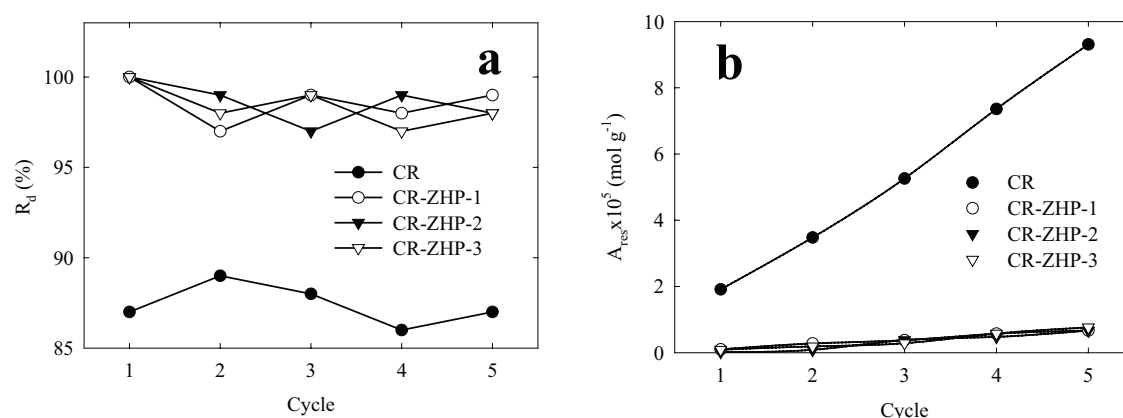


Fig. 12. Regeneration degree of the ion-exchangers (a) and residual content of UO_2^{2+} in ion-exchangers (b) from cycle to cycle of sorption-regeneration.

3.8. Regeneration

Composite ion-exchangers demonstrate higher regeneration degree under batch conditions than unmodified resin (Fig. 12(a)). The (A_{res}) was calculated as:

$$A_{res} = \sum_{i=1}^i A_i \frac{R_{d,i}}{100\%} \quad (14)$$

Here i is a number of cycle of sorption-regeneration. Contrary to the composites, the residual capacity of the CR sample grows rapidly from cycle to cycle of regeneration indicating a possibility to lose ability to sorb UO_2^{2+} rather soon (Fig. 12(b)).

Since ZHP is related to weakly acidic ion-exchanger [17,18,28], increasing of its content in the polymer provides more significant UO_2^{2+} desorption (see Table 4).

4. Conclusions

Insertion of ZHP particles into the ion-exchange polymer changes its porous structure and influences ion exchange properties of the resin. The particles provide swelling pressure in the polymer pores, which are free from $-SO_3$ groups. In opposite to unmodified resin, isotherms of UO_2^{2+} sorption obey the D-R model within a wider interval of solution concentration. The composites require less amount of reagents for regeneration, than the polymer. One-time treatment of the composites with a 1 M H_2SO_4 solution causes complete UO_2^{2+} desorption, then the samples can be used repeatedly.

The inorganic particles of micron size, which occupy structure defects, are characterized by the largest amount of phosphorus (CR-ZHP-2). Since the largest particles increase swelling pressure, they can be formally considered as a cross-linking agent. However, the effective diffusion coefficient for $UO_2^{2+} \rightarrow H^+$ exchange is approximately three times higher than that for unmodified resin. This can be explained by an increase of distance between functional groups of the polymer constituent, which is affected by ZHP. The CR-ZHP-2 sample demonstrates the highest breakthrough capacity towards UO_2^{2+} species, when they are removed from water containing also hardness ions.

In the case of CR-ZHP-1 and CR-ZHP-3 samples, which contain ZHP particles mainly in voids between gel

regions, $UO_2^{2+} \rightarrow H^+$ exchange is complicated by chemical reaction similarly to the inorganic ion-exchanger – sorption is affected mainly by the inorganic constituent. This is evidently caused by partial exclusion of $-SO_3$ groups from ion exchange due to squeezing of clusters and channels. In order to avoid this, the particles in transport pores are assumed to be necessary. This can be evidently reached by temperature control of ZHP deposition.

Further improvement of sorption affinity of the composites towards UO_2^{2+} can be achieved not only by regulation of size and location of ZHP particles but also by increasing of phosphorus content in the inorganic constituent.

Acknowledgements

The work was supported by projects within the framework of programs supported by the National Academy of Science of Ukraine “Fundamental problems of creation of new materials for chemical industry” (Grant No. 49/12).

References

- [1] C. Gupta, H. Singh, Uranium Resource Processing: Secondary Resources, Springer-Verlag, Berlin, Heidelberg, New York, 2003.
- [2] V.I. Ferronsky, V.A. Polyakov, Isotopes of the Earth's Hydrosphere, Springer, Dordrecht, Geidelberg, London, New York, 2012.
- [3] W. Brine, The toxicity of depleted uranium, Int. J. Environ. Res. Public Health, 7 (2010) 303–313.
- [4] B. Hua, H. Xu, J. Terry, B. Deng, Kinetics of uranium (VI) reduction by hydrogen sulfide in anoxic aqueous systems, Environ. Sci. Technol., 40 (2006) 4666–4671.
- [5] S.S. Sandhu, K.B. Kohli, A.S. Brar, Photochemical reduction of the uranyl ion with dialkyl sulfides, Inorg. Chem., 23 (1984) 3609–3612.
- [6] D.S. Alessi, J.S. Lezama-Pacheco, N. Janot, E.I. Suvorova, J.M. Cerrato, D.E. Giammar, J.A. Davis, P.M. Fox, K.H. Williams, P.E. Long, K.M. Handley, R. Bernier-Latmani, J.R. Bargar, Speciation and reactivity of uranium products formed during in situ bioremediation in a shallow alluvial aquifer, Environ. Sci. Technol., 48 (2014) 12842–12850.
- [7] E.J. Zaganari, Ion Exchange Resins in Uranium Hydrometallurgy, Books on Demand France, Paris, 2009.
- [8] I.V. Pylypenko, I.A. Kovalchuk, B. Yu. Kornilovich, Synthesis and sorption properties of Ti- and Ti/Al-pillared montmorillonite, Khim. Fiz. Technol. Poverhni., 6 (2015) 336–342.

- [9] C.D. Barnes, R.A. Da Silva Neves, M. Streat, Anion exchange of uranium from aqueous sulphuric acid solutions: diffusion kinetics, *J. Appl. Chem. Biotechnol.*, 24 (1974) 787–801.
- [10] A. Kadous, M.A. Didi, D. Villemin, Removal of uranium(VI) from acetate medium using Lewatit TP 260 resin, *J. Radioanal. Nucl. Chem.*, 288 (2011) 553–561.
- [11] N.A. Yaroshenko, V.F. Sazonova, O.V. Perlova, N.A. Perlova, Sorption of uranium compounds by zirconium-silica nanosorbents, *Russ. J. Appl. Chem.* 85 (2012) 849–855.
- [12] O.V. Perlova, V.F. Sazonova, N.A. Perlova, N.A. Yaroshenko, Kinetics of sorption of uranium(VI) compounds with zirconium-silica nanosorbents, *Russ. J. Phys. Chem. A.*, 88 (2014) 1012–1016.
- [13] W.I. Zidan, M.M. Abo-Aly, O.A. Elhefnawy, E. Bakier, Batch and column studies on uranium adsorption by Amberlite XAD-4 modified with nano-manganese dioxide, *J. Radioanal. Nucl. Chem.*, 304 (2015) 645–653.
- [14] A. Kimaro, L.A. Kelly, G.M. Murray, Synthesis and characterization of molecularly imprinted uranyl ion exchange resins, *Separ. Sci. Technol.*, 40 (2005) 2035–2052.
- [15] A. Rahmati, A. Ghaemi, M. Samadfam, Kinetic and thermodynamic studies of uranium(VI) adsorption using Amberlite IRA-910 resin, *Annals Nucl. Energy*, 39 (2012) 42–48.
- [16] T.S. Anirudhan, P.G. Radhakrishnan, Kinetics, thermodynamics and surface heterogeneity assessment of uranium(VI) adsorption onto cation exchange resin derived from a lignocellulosic residue, *Appl. Surf. Sci.*, 255 (2009) 4983–4991.
- [17] N.A. Nekrasova, V.M. Gelis, V.V. Milyutin, N.A. Budantseva, E.A. Kozliti, M.V. Logunov, Yu. E. Pristinskii, Sorption of Th, U, and Am on phosphorus-containing ion-exchange materials, *Radiochem.*, 52 (2010) 71–75.
- [18] O.I. Zakutevskiy, T.S. Psareva, V.V. Strelko, Sorption of U(VI) ions on sol-gel-synthesized amorphous spherically granulated titanium phosphates, *Russ. J. Appl. Chem.*, 85 (2012) 1366–1370.
- [19] Yu. S. Dzyazko, L.N. Ponomaryova, Yu. M. Volkovich, V.E. Sosenkin, V.N. Belyakov, Polymer ion-exchangers modified with zirconium hydrophosphate for removal of Cd²⁺ ions from diluted solutions, *Separ. Sci. Technol.*, 48 (2013) 2140–2149.
- [20] Yu. S. Dzyazko, Y.M. Volkovich, L.N. Ponomaryova, V.E. Sosenkin, V.V. Trachevskii, V.N. Belyakov, Composite ion-exchangers based on flexible resin containing zirconium hydrophosphate for electromembrane separation, *J. Nanosci. Technol.*, 2 (2016) 43–49.
- [21] Yu. S. Dzyazko, L.N. Ponomaryova, Yu. M. Volkovich, V.V. Trachevskii, A.V. Palchik, Ion-exchange resin modified with aggregated nanoparticles of zirconium hydrophosphate. Morphology and functional properties, *Micropor. Mesopor. Mater.*, 198 (2014) 55–62.
- [22] Yu. S. Dzyazko, L.N. Ponomaryova, L.M. Rozhdestvenskaya, S.L. Vasilyuk, V.N. Belyakov, Electrodeionization of low-concentrated multicomponent Ni²⁺-containing solutions using organic-inorganic ion-exchangers, *Desalination*, 342 (2014) 52–60.
- [23] Yu. S. Dzyazko, L.N. Ponomareva, Y.M. Volkovich, V.E. Sosenkin, Effect of the porous structure of polymer on the kinetics of Ni²⁺ exchange on hybrid inorganic-organic ionites, *Russ. J. Phys. Chem. A*, 86 (2012) 913–919.
- [24] Yu. S. Dzyazko, L.N. Ponomareva, Y.M. Volkovich, V.E. Sosenkin, V.N. Belyakov, Conducting properties of a gel ionite modified with zirconium hydrophosphate nanoparticles, *Russ. J. Electrochem.*, 49 (2013) 209–215.
- [25] S. Sarkar, P.K. Chatterjee, L. Cumbal, A.K. Sen Gupta, Hybrid ion exchanger supported nanocomposites: sorption and sensing for environmental applications, *Chem. Eng. J.*, 166 (2011) 923–931.
- [26] B.C. Pan, Q.R. Zhang, W.M. Zhang, B.J. Pan, W. Du, L. Lu, Q.J. Zhang, Z.W. Xu, Q.X. Zhang, Highly effective removal of heavy metals by polymer-based zirconium phosphate: a case study of lead ion, *J. Colloid Interface Sci.*, 310 (2007) 99–105.
- [27] Q. Zhang, B. Pan, S. Zhang, J. Wang, W. Zhang, L. Lu, New insights into nanocomposite adsorbents for water treatment: a case study of polystyrene-supported zirconium phosphate nanoparticles for lead removal, *J. Nanopart. Res.*, 13 (2011) 5355–5364.
- [28] Yu. Dzyazko, L. Rozhdestvenska, A. Palchik, F. Lapique, Ion-exchange properties and mobility of Cu²⁺ ions in zirconium hydrophosphate ion exchangers, *Separ. Purif. Technol.*, 45 (2005) 141–146.
- [29] Yu. M. Volkovich, V.S. Bagotzky, The method of standard porosimetry – 1. Principles and possibilities, *J. Power Sources*, 48 (1994) 327–338.
- [30] Yu. M. Volkovich, V.E. Sosenkin, Porous structure and wetting of fuel cell components as the factors determining their electrochemical characteristics, *Russ. Chem. Rev.*, 81 (2012) 936–959.
- [31] Yu. M. Volkovich, V.S. Bagotzky, Experimental Methods for Investigation of Porous Materials and Powders, Yu. M. Volkovich, A.N. Filippov, V.S. Bagotzky, Eds., *Porous Materials and Powders Used in Different Fields of Science and Technology*, Springer-Verlag, London, 2014, pp. 1–8.
- [32] J. Rouquerol, G. Baron, R. Denoyel, H. Giesche, J. Groen, P. Klobes, P. Levitz, A.V. Neimark, S. Rigby, R. Skudas, K. Sing, M. Thommes, K. Unger, Liquid intrusion and alternative methods for the characterization of macroporous materials (IUPAC Technical Report), *Pure Appl. Chem.*, 84 (2012) 107–136.
- [33] Z. Zhu, Y. Pranolo, C.Y. Cheng, Separation of uranium and thorium from rare earths for rare earth production – a review, *Miner. Eng.*, 77 (2015) 185–196.
- [34] B.V. Kadam, B. Maiti, R.M. Sathe, Selective spectrophotometric method for the determination of uranium(VI), *Analyst*, 106 (1981) 724–726.
- [35] A.S. Myerson, *Handbook of Industrial Crystallization*, Butterworth-Heinemann, Woburn, 2002.
- [36] I. Nicotera, A. Khalfan, G. Goenaga, T. Zhang, A. Bocarsly, S. Greenbaum, NMR investigation of water and methanol mobility in nanocomposite fuel cell membranes, *Ionics*, 14 (2008) 243–253.
- [37] Yu. S. Dzyazko, Yu. M. Volkovich, V.E. Sosenkin, N.F. Nikolskaya, Yu. P. Gomza, Composite inorganic membranes containing nanoparticles of hydrated zirconium dioxide for electro-dialytic separation, *Nanoscale Res. Lett.*, 9 (2014) 271.
- [38] V.Y. Nimon, S.J. Visco, L.C. De Jonghe, Y.M. Volkovich, D.A. Bograchev, Modeling and experimental study of porous carbon cathodes in Li-O₂ cells with non-aqueous electrolyte, *Electrochem. Lett.*, 2 (2013) A33-A36.
- [39] N.P. Berezina, Yu. M. Volkovich, N.A. Kononenko, I.A. Blinov, Water distribution studies in heterogeneous ion-exchange membranes by standard porosimetry, *Soviet Electrochem.*, 23 (1987) 858–862.
- [40] Yu. Dzyazko, L. Rozhdestveskaya, Yu. Zmievskii, Yu. Volkovich, V. Sosenkin, N. Nikolskaya, S. Vasilyuk, V. Myronchuk, V. Belyakov, Heterogeneous membranes modified with nanoparticles of inorganic ion-exchangers for whey demineralization, *Mater. Today: Proceedings*, 2 (2015) 3864–3873.
- [41] F. Helfferich, *Ion Exchange*, Dover, New York, 1995.
- [42] N.P. Berezina, N.A. Kononenko, O.A. Dyomina, N.P. Gnusin, Characterization of ion-exchange membrane materials: properties vs. structure, *Adv. Colloid Interface Sci.*, 139 (2008) 3–28.
- [43] G. Gapel, Speciation of Actinides, R. Cormelis, J.A. Caruso, H. Crews, K.G. Heumann, Eds., *Handbook of Elemental Speciation II. Species in the Environment, Food, Medicine and Occupational Health*, Wiley, Chichester, 2005, pp. 509–563.
- [44] G.E. Boyd, A.W. Adamson, P.P. Mayers, The exchange adsorption of ions from aqueous solutions by organic zeolites. 2. Kinetics, *J. Amer. Chem. Soc.*, 69 (1947) 2836–2848.
- [45] S. Lagergren, About the theory of so called adsorption of soluble substances, *Kungliga Svenska Vetenskapsakademiens Handlingar*, 24 (1898) 1–39.
- [46] Y.S. Ho, G. McKay, Pseudo-second-order model for sorption processes, *Process Biochem.*, 34 (1999) 451–465.
- [47] Yu. S. Dzyazko, V.V. Trachevskii, L.M. Rozhdestvenskaya, S.L. Vasilyuk, V.N. Belyakov, Interaction of sorbed Ni(II) ions with amorphous zirconium hydrogen phosphate, *Russ. J. Phys. Chem. A*, 87 (2013) 840–845.
- [48] W. Riemann, H. Walton, *Ion Exchange in Analytical Chemistry*, Pergamon Press, Oxford, New York, Toronto, Sydney, Braunschweig, 1970.